

COMPLEXITY-BASED RULES FOR THE CONCEPTUAL DESIGN OF ROBOTIC ARCHITECTURES

Waseem A. Khan, Stéphane Caro, Damiano Pasini, Jorge Angeles

Department of Mechanical Engineering

McGill University

817, Sherbrooke St. West

Montreal, QC, Canada, H3A 2K6

{wakhan, caro}@cim.mcgill.ca, damiano.pasini@mcgill.ca, angeles@cim.mcgill.ca

Abstract We propose a formulation capable of measuring the complexity of kinematic chains at the conceptual stage in robot design. First, the complexity of the three basic lower kinematic pairs, the revolute, the prismatic and the cylindrical pairs, is proposed. Then, a formulation of the complexity of kinematic chains is introduced. Next, the complexity of the basic displacement subgroups generated by the lower kinematic pairs is established. Finally, as an example, two realizations of the Schönflies displacement subgroup are compared.

Keywords: Conceptual design, complexity, kinematic chains, displacement subgroups

1. Introduction

We propose here a formulation capable of measuring the complexity of the kinematic chains of robotic architectures at the conceptual-design stage. The motivation lies in providing an aid to the robot designer when selecting the best design alternative among various candidates at the early stages of the design process, when a parametric design is not yet available. Complexity has been recognized as a major issue in design engineering (Suh, 2005), although a theoretical framework aimed at its application to design is still lacking.

In this paper, the complexity of the three basic lower kinematic pairs, the revolute, the prismatic and the cylindrical pairs, is obtained. Then, a formulation to measure the complexity of kinematic bonds is introduced. Based on this formulation, the complexity of the six displacement subgroups is established. Finally, as an application, two realizations of the Schönflies displacement subgroup (Angeles, 2004; Company et al., 2001) are compared.

2. Kinematic Pair, Kinematic Bond and Kinematic Chain

A *kinematic bond* is defined as a set of displacements stemming from a product of displacement subgroups, (Hervé, 1978; Angeles, 2004). Notice that a bond itself need not be a subgroup. We denote a kinematic bond by $\mathcal{L}(i, n)$, where i and n stand for the integer numbers associated with the two end links of the bond. There are six basic displacement subgroups $\mathcal{R}(\mathcal{A})$, $\mathcal{P}(\mathbf{e})$, $\mathcal{H}(\mathcal{A}, p)$, $\mathcal{C}(\mathcal{A})$, $\mathcal{F}(\mathbf{u}, \mathbf{v})$ and $\mathcal{S}(O)$ (Hervé, 1978; Hervé, 1999; Angeles, 2004). In this notation, \mathcal{A} stands for the axis of the kinematic pair in question; \mathbf{e} , \mathbf{u} and \mathbf{v} are unit vectors, O is a point denoting the center of the spherical pair; and p is the pitch of the helical pair.

A kinematic bond is realized by a *kinematic chain*. A kinematic chain is the result of the coupling of rigid bodies, called links via *kinematic pairs*. When the coupling takes place in such a way that the two links share a common surface, a *lower kinematic pair* results; when the coupling takes place along a common line or a common point, a *higher kinematic pair* is obtained. Examples of higher kinematic pairs include gears and cams. For the sake of brevity, we will restrict ourselves to the lower kinematic pairs and will consider only those forms in which the contact is maintained by the wrapping action of the conjugate surfaces. The inclusion of higher kinematic pairs can be done based on the similar approach that we take in this paper.

There are six basic lower kinematic pairs, namely (1) revolute R, (2) prismatic P, (3) helical H, (4) cylindrical C, (5) planar F, and (6) spherical S. These pairs are the generators of the displacement subgroups $\mathcal{R}(\mathcal{A})$, $\mathcal{P}(\mathbf{e})$, $\mathcal{H}(\mathcal{A}, p)$, $\mathcal{C}(\mathcal{A})$, $\mathcal{F}(\mathbf{u}, \mathbf{v})$ and $\mathcal{S}(O)$, respectively. Although the displacement subgroups can be realized by their corresponding lower kinematic pairs, it is usually possible to realize the displacement subgroups by appropriate kinematic chains. A common example is that of the $\mathcal{C}(\mathcal{A})$ which, besides C pair, could be realized by a suitable concatenation of a P and a R pair.

3. The Loss of Regularity of a Surface

In this section, we propose a measure of the irregularities in a given surface. In this vein, we define the *loss of regularity LOR* as

$$LOR \equiv l \frac{\|\kappa'_{rms}\|_2}{\|\kappa_{rms}\|_2} \quad (1)$$

where κ_{rms} is the root mean square of the two principal curvatures at a point of the surface, κ'_{rms} is the derivative of κ_{rms} with respect to a suit-

able length parameter s , and l is a suitable homogenizing length. The loss of regularity is inspired from the Taguchi's *loss function* (Taguchi, 1993) and measures the diversity of the curvature distribution of the given surface. In the following sub-sections we evaluate the loss of regularity of the surfaces associated with the lower kinematic pairs.

3.1 Loss of regularity of the surface of the R pair

Typically, the surface associated with the revolute pair is assumed to be that of a cylinder. However, in order to realize a $\mathcal{R}(\mathcal{A})$ subgroup, the translation motion in the axial direction of the cylindrical surface must be constrained. This calls for additional surfaces, which must then be blended smoothly with the cylindrical surface in order to avoid curvature discontinuities.

The above discussion reveals that the surface associated with a revolute pair has to be a surface of revolution and cannot be an extruded surface; the cylindrical surface is both. We should thus look for a generatrix $P(x)$ other than a straight line but with zero curvature at both ends. The latter constraint would allow a shaft of appropriate diameter to be blended smoothly on both ends. We thus have the following seven constraints

$$\begin{aligned} P(-1) &= 0; & P'(-1) &= 0; & P''(-1) &= 0; \\ P(0) &= 1; & P(1) &= 0; & P'(1) &= 0; & P''(-1) &= 0. \end{aligned}$$

A sixth degree polynomial is thus required to meet the above mentioned constraints. Solving for the coefficients, we obtain the equation of the generatrix $P(x)$ as

$$P(x) = -x^6 + 3x^4 - 3x^2 + 1.0 \quad (2)$$

Figure 1(a) shows a plot of $P(x)$, while Fig. ?? is a 3-D rendering of the surface S_R obtained by revolving the generatrix P about the x-axis.

The two principal curvatures for the surface under study are given by (Oprea, 2004)

$$\kappa_\mu = \frac{-y''}{(1 + y'^2)^{3/2}} \quad (3)$$

$$\kappa_\pi = \frac{1}{y(1 + y'^2)^{1/2}} \quad (4)$$

where $y = P + r$ and r is the radius of the shaft.

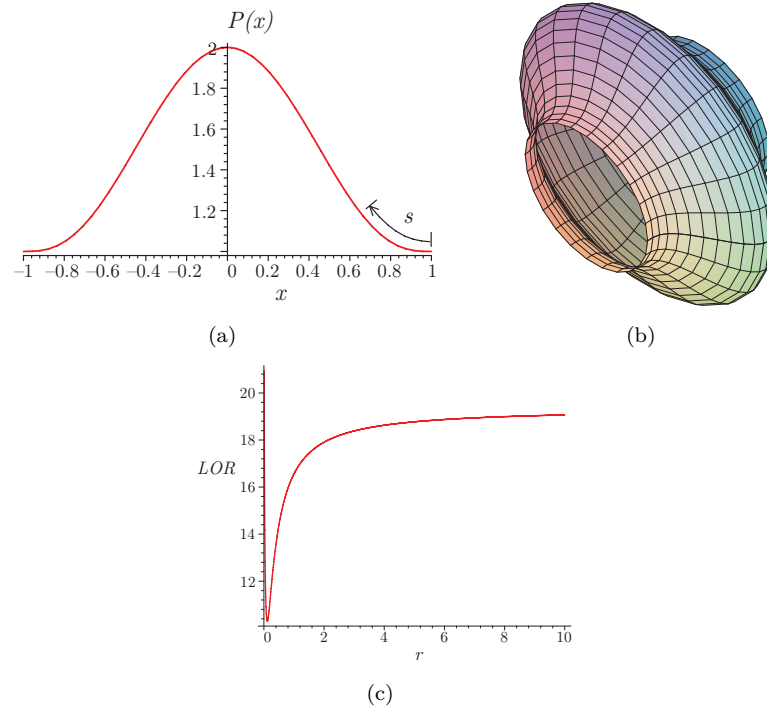


Figure 1. (a) Generatrix of the revolute pair, (b) 3-D rendering of the surface of revolution and (c) LOR vs. shaft radius r

The root mean square of the two principal curvatures, κ_μ and κ_π , can now be obtained, i.e.,

$$\kappa_{rms} = \sqrt{\frac{1}{2}(\kappa_\mu^2 + \kappa_\pi^2)} \quad (5)$$

Next, we need to choose a suitable length parameter s and the homogenizing length l . A natural choice for s is the distance travelled along the generatrix (Fig. 1(a)); that for l is the total length of the generatrix.

The loss of regularity of S_R can now be evaluated by using eq.(1). Figure 1(c) is a graph between loss of regularity of S_R and the radius of the shaft r . Notice that the loss of regularity of S_R is not monotonic in r . Further, the loss of regularity of S_R reaches a steady-state value of 19.3571. We thus assign the loss of regularity of the surface associated with the revolute pair as $LOR_R = 19.3571$.

3.2 Loss of regularity of the surface of the P pair

The most common cross section of a P pair is a dove tail, but could well be an ellipse, a square or a rectangle. A family of smooth curves that continuously leads from a circle to a rectangle is known as Lamé curves (Gardner, 1965)¹. In their simplest form, these curves are given by

$$x^m + y^m = 1 \tag{6}$$

where $m > 0$ is an even integer. When $m = 2$, the corresponding curve is a circle of unit radius, with its center at the origin of the x - y plane. As m increases, the curve becomes flatter and flatter at its intersections with the coordinate axes, becoming more like a square. For $m \rightarrow \infty$, the curve is a square of sides equal to two units of length and centered at the origin. A Fourier analysis based on the curvature of these curves confirms the intuitively accepted notion that the spectral richness, or diversity, of the curvature increases with m (Khan, Caro, Pasini and Angeles, 2006).

The loss of regularity of the surface of the prismatic pair obtained by extruding a square or a rectangle is expected to have a very high value. A Lamé curve L with $m = 4$ is perhaps the best candidate for the cross section of the prismatic pair. This curve is shown in Fig. 2(a). Figure ?? is a 3-D rendering of the surface S_P obtained by extruding L along the z -axis.

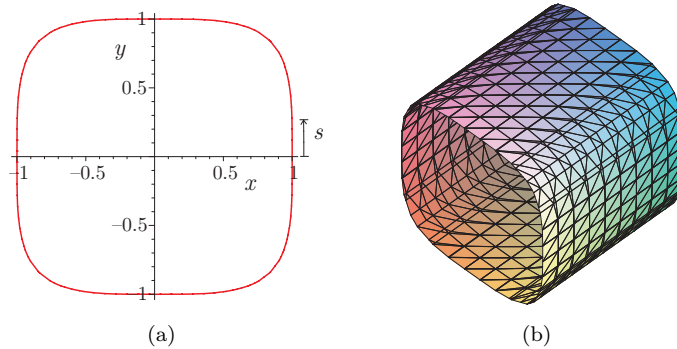


Figure 2. (a) Cross section of the prismatic pair, (b) 3-D rendering of the extruded surface

The two principal curvatures for S_P are given by

$$\kappa_\mu = \frac{x''y' - y''x'}{(x'^2 + y'^2)^{3/2}} \tag{7}$$

$$\kappa_\pi = 0 \tag{8}$$

The root mean square of the two principal curvatures, κ_μ and κ_π thus reduces to

$$\kappa_{rms} = \kappa_\mu \tag{9}$$

The length parameter s and the homogenizing length l are correspondingly the distance travelled along the curve under study (Fig. 2(a)), and the total length of the curve.

The loss of regularity LOR_P obtained for the surface S_P associated with the P pair is $LOR_P = 19.6802$.

3.3 Loss of regularity of the surface of the F pair

The F pair is a generator of the planar subgroup \mathcal{F} and requires two parallel planes, separated by an arbitrary distance. In order to avoid corners and edges, a suitable ‘blending option’ is the use of the quartic Lamé curve. The concept is shown in Fig. 3(a) while a 3-D rendering of the same is shown in Fig. ???. Notice that the female member of the pair is an extrusion surface P_{Fm} while the male member is a solid of revolution S_{Fm} .

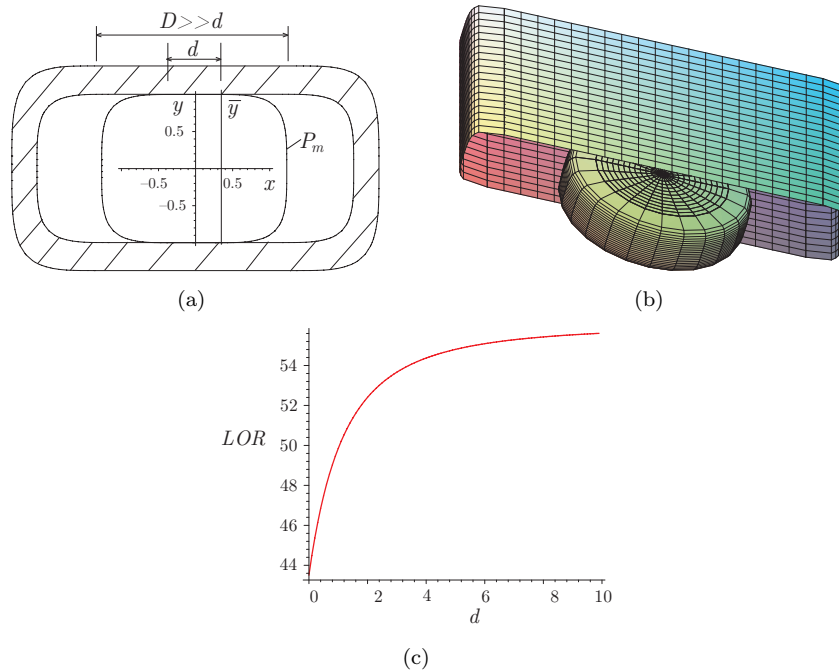


Figure 3. (a) Cross section of the planar pair, (b) 3-D rendering of the surface of the planar pair and (c) LOR vs. flat diameter of the male member r

The loss of regularity for the planar pair is contributed by both; the male and the female member.

Further, a flat surfaces does not contribute the loss of regularity. A plane is a sphere of an infinite radius. We thus obtain

$$LOR_{\text{plane}} = \lim_{\kappa \rightarrow 0} \frac{\|\kappa'_{rms}\|_2}{\|\kappa_{rms}\|_2} = l \lim_{\kappa \rightarrow 0} \frac{0}{\|\kappa_{rms}\|_2} = 0 \quad (10)$$

The loss of regularity of the female member LOR_{Ff} is thus the same as that of the prismatic pair.

The loss of regularity of the male member LOR_{Fm} is evaluated as follows. The two principal curvatures at a point of the surface S_{Fm} are given by

$$\begin{aligned} \kappa_\mu &= \frac{x''y' - y''x'}{(x'^2 + y'^2)^{3/2}} \\ \kappa_\pi &= \frac{1}{x\sqrt{1+x'^2}} \end{aligned} \quad (11)$$

where $x = P_m(y) + d/2$, P_m is the distance of the generatrix from the \bar{y} and d is the diameter of the flat surface as shown in the Fig. 3(a).

The length parameter s and the homogenizing length l are correspondingly the distance travelled along the generatrix P_m (Fig. 3(a)) and the its total length.

Figure 3(c) is a graph between loss of regularity of S_{Fm} and the diameter of the flat d . Notice that the loss of regularity of S_{Fm} for this case is monotonic in d . Further, the loss of regularity of S_{Fm} reaches steady-state value of approximately 56.0399. We thus assign the loss of regularity of the surface associated with the male member of the F pair as $LOR_{Ff} = 56.0399$

Finally, the LOR_F is the mean of the loss of regularity of the male and the female members, i.e., $LOR_F = (LOR_{Ff} + LOR_{Fm})/2 = 37.8601$.

3.4 Loss of regularity of the surface of the C and S pair

The root mean square of the principal curvatures of the cylindrical and that of the spherical surface is a constant. Hence, the loss of regularity is zero for the both surfaces, i.e., $LOR_C = LOR_S = 0$.

4. The Geometric Complexity of Lower Kinematic Pairs

In this section we introduce the *geometric complexity* of the lower kinematic pairs based on the loss of regularity introduced earlier. In

Table 1. Geometric complexity of the five basic displacement subgroups

Description	Loss of regularity			Geometric complexity
	male	female	mean	K_G
R	19.3571	19.3571	19.3571	0.6919
C	0	0	0	0
P	19.6802	19.6802	19.6802	0.6979
F	56.0399	19.6802	37.8601	0.9
S	0	0	0	0
$q = -\ln(0.1)/36.8601 = 0.0608$				

this vein, we define the geometric complexity $K_{G|x}$ of a pair x as

$$K_{G|x} \equiv 1 - \exp(-q_G LOR_x) \quad (12)$$

where LOR_x is the loss of regularity of the surface associated with the pair x and q_G is the resolution factor that would assign a geometric complexity of 0.9 to the pair with maximum loss of regularity, i.e.,

$$q_G = \begin{cases} -\ln(0.1)/LOR_{\max} & LOR_{\max} > 0; \\ 0 & LOR_{\max} = 0. \end{cases}$$

The geometric complexity of the lower kinematic pairs is tabulated in Table 1.

5. The Complexity of Kinematic Bonds

In this section we lay the foundations for the evaluation of the complexity of any kinematic bond. In this vein, we first restrict our study to kinematic bonds that are realizable using lower kinematic pairs; the study of bonds including higher kinematic pairs is as yet to be completed. Next, we define the complexity $K \in [0, 1]$ of a kinematic chain as a *convex combination* (Boyd, 2004) of its various complexities, namely,

$$K = w_J K_J + w_N K_N + w_L K_L + w_B K_B \quad (13)$$

where $K_J \in [0, 1]$ is the joint-type complexity, $K_N \in [0, 1]$ the joint-number complexity, $K_L \in [0, 1]$ the loop-complexity, and $K_B \in [0, 1]$ the bond-realization complexity. Furthermore, w_J , w_N , w_L , and w_B denote their corresponding non-negative weights, such that $w_J + w_N + w_L + w_B = 1$.

5.1 Joint-type complexity K_J

Joint-type complexity is that associated with the type of LKPs used in a kinematic chain. For the time being, we take the geometric complexity

$K_G|x$ of the x pair as the joint type complexity $K_{J|x}$. We define the joint-type complexity K_J of a kinematic bond as

$$K_{J|x} = \frac{1}{n}(n_R K_{J|R} + n_P K_{J|P} + n_C K_{J|C} + n_F K_{J|F} + n_S K_{J|S}) \quad (14)$$

where n_R , n_P , n_C , n_F and n_S are the number of revolute, prismatic, cylindrical, planar and spherical joints, respectively, while n is the total number of pairs.

5.2 Joint-number complexity K_N

The joint-number complexity K_N is defined as that associated with a kinematic bond x by virtue of its number of kinematic pairs, with respect to the minimum required to realize the same set of displacements. We propose the expression

$$K_{N|x} = 1 - \exp(-q_N N); \quad N = n - m \quad (15)$$

where n is the number of joints used in the realization of the bond x , m is the minimum number of LKPs required to produce a displacement of bond x , and q_N is a *resolution parameter*, to be adjusted according to the resolution required. Note that $K_{N|x} \in [0, 1]$.

5.3 Loop-complexity K_L

The loop-complexity K_L of a kinematic bond is that associated with the number of independent loops of the kinematic chain connecting the two links, i and n , of a kinematic bond x , with respect to the minimum required to produce the prescribed displacement set. The loop-complexity can be evaluated by means of the formula:

$$K_{L|x} = 1 - \exp(-q_L L); \quad L = l - d \quad (16)$$

where l is the number of kinematic loops, d is the minimum number of loops required to realize such a bond and q_L is a normalizing factor.

5.4 Bond-realization complexity K_B

The bond-realization complexity is associated with the geometric constraints involved in the realization of a kinematic bond. The complexity of geometric constraints may be evaluated by *the number of floating-point operations (flops) required to realize a geometric constraint*. One flop is customarily defined as the combination of one addition and one multiplication.

Table 2. Verification cost of some geometric constraints

Geometric constraint	Verification	flops	total flops
Intersection of two lines	$(\mathbf{e}_1 \times \mathbf{e}_2) \cdot \mathbf{q}_{21} = 0$	$5A + 9M$	9
Angle of intersection	$\mathbf{e}_1 \cdot \mathbf{e}_2 = \cos \alpha$	$2A + 3M$	3
Parallelism b/w two lines	$\mathbf{e}_1 \times \mathbf{e}_2 = \mathbf{0}_3$	$3A + 6M$	6
Length of common normal	$\ \mathbf{q}_{21} - (\mathbf{q}_{21} \cdot \mathbf{e}_1) \mathbf{e}_1\ _2^2 = d^2$	$7A + 9M$	9
Intersection of three lines	$\det(\mathbf{C}) = 0$	$30A + 36M$	36
$\mathbf{e}_1, \mathbf{e}_2$ and \mathbf{e}_3 span 3D space	$\det([\mathbf{e}_1 \ \mathbf{e}_2 \ \mathbf{e}_3]) \neq 0$	$5A + 9M$	9

Lack of space prevents us from including the flop analysis of the geometric constraints, which is reported in (Khan, Caro, Pasini and Angeles, 2006). A summary of the results of this analysis is displayed in Table 2.

The bond-realization complexity based on the geometric constraints of its realization can now be defined as

$$K_B = 1 - \exp(-q_B f) \quad (17)$$

where f is the number of floating point operations corresponding to the constraints, q_B being another resolution parameter.

Definition of the resolution parameters. Three resolution parameters, namely q_N , q_L and q_B were introduced above. These parameters set an appropriate resolution for the complexity at hand. Since the foregoing formulation is intended to compare the complexities of two or more kinematic chains, it is reasonable to assign a complexity of 0.9 to the chain with maximum complexity and evaluate the normalizing constant from there, i.e., for $J = B, L, N$,

$$q_J = \begin{cases} -\ln(0.1)/J_{\max} & J_{\max} > 0; \\ 0 & J_{\max} = 0. \end{cases}$$

6. Complexity of the Basic Displacement Subgroups

In Section 5.1, we assigned the joint-type complexity of the lower kinematic pairs as the geometric complexity of the surface associated with the lower kinematic pairs.

The F pair requires the machining of two parallel planes, separated by an arbitrary distance. Further, the F pair exhibits accessibility problem to the male member of the coupling. The F pair is not used in common practice.

Further, precision spherical pairs are expensive and difficult to manufacture.

Table 3. Complexity of the six basic displacement subgroups

Subgroup	Desc.	K_J	K_N	K_B	K
$\mathcal{R}(\mathcal{A})$	R	0.6919/1	$1 - e^{-q_N(0)}$	$1 - e^{-q_B(0)}$	0.2306
$\mathcal{P}(\mathbf{e})$	P	0.6979/1	$1 - e^{-q_N(0)}$	$1 - e^{-q_B(0)}$	0.2326
$\mathcal{C}(\mathcal{A})$	C	0/1	$1 - e^{-q_N(0)}$	$1 - e^{-q_B(0)}$	0
	PR	1.3898/2	$1 - e^{-q_N(1)}$	$1 - e^{-q_B(6)}$	0.5476
	PPR	2.0877/3	$1 - e^{-q_N(2)}$	$1 - e^{-q_B(12)}$	0.6849
$\mathcal{F}(\mathbf{u}, \mathbf{v})$	RRR	2.0757/3	$1 - e^{-q_N(2)}$	$1 - e^{-q_B(12)}$	0.6835
	RPR	2.0817/3	$1 - e^{-q_N(2)}$	$1 - e^{-q_B(9)}$	0.6543
$\mathcal{S}(O)$	RRR	2.0757/3	$1 - e^{-q_N(2)}$	$1 - e^{-q_B(45)}$	0.8306

$$q_N = -\ln(0.1)/2 = 1.1513; \quad q_B = -\ln(0.1)/45 = 0.0512$$

Hence, using the geometric complexity of the LKPs as the corresponding joint-type complexities is not justified. In order to solve this problem we must resort back to the complexity of the displacement subgroups.

The basic displacement subgroups can be realized either by their corresponding pairs or by a kinematic chain: the kinematic chain is a serial array of lower kinematic pairs. The complexity of the displacement subgroups is defined as the complexity of the realization that exhibits the minimum kinematic bond complexity (Section).

The complexity of the six displacement subgroups generated by the lower kinematic pairs can now be evaluated. In this vein, we apply the formulation introduced in the previous section to different realizations of the displacement subgroups under study. Table 3 displays some pertinent realizations. The minimum complexity values found for $\mathcal{R}(\mathcal{A})$, $\mathcal{P}(\mathbf{e})$, $\mathcal{C}(\mathcal{A})$, $\mathcal{F}(\mathbf{u}, \mathbf{v})$ and $\mathcal{S}(O)$ are, correspondingly, 0.2306, 0.2326, 0, 0.6835 and 0.8306 and . Normalizing the above results, we obtain the complexities of the basic displacement subgroups as

$$K_{J|R} = 0.2776, \quad K_{J|P} = 0.2801, \quad K_{J|C} = 0, \quad K_{J|F} = 0.8229, \quad K_{J|S} = 1.0 \tag{18}$$

Notice that, although these are not the joint-type complexity values as defined in Section 6, which are rather based on *form* than on *function*, the above values can still be used to evaluate the joint-type complexity in eq.(14).

7. Example: Complexity Analysis of Two Realizations of the Schönflies Subgroup $\mathcal{X}(\mathbf{e})$

We apply our proposed formulation to compute the complexity of two Schönflies-motion generators. The motion capability of this subgroup

Table 4. Complexity of two realizations of the $\mathcal{X}(\mathbf{e})$ subgroup

Description	K_J	K_N	K_L	K_B	K
McGill SMG	14.5299/21	$1 - e^{-q_N(21-2)}$	$1 - e^{-q_L(5-0)}$	$1 - e^{-q_B(258)}$	0.7179
H4	20.1514/22	$1 - e^{-q_N(22-2)}$	$1 - e^{-q_L(7-0)}$	$1 - e^{-q_B(99)}$	0.7971
$q_N = -\ln(0.1)/20 = 0.1151; q_L = -\ln(0.1)/7 = 0.3289; q_B = -\ln(0.1)/258 = 0.0089$					

includes three independent translations and one rotation about an axis of fixed orientation. Figure 4(b) shows the joint and loop graphs of the McGill SMG (Angeles, 2005) and the H4 robot (Company et al., 2001).

Table 4 displays the different complexity values associated with the topology of the two robots. Here, we note that the overall complexity of the McGill SMG is lower than that of the H4 robot.

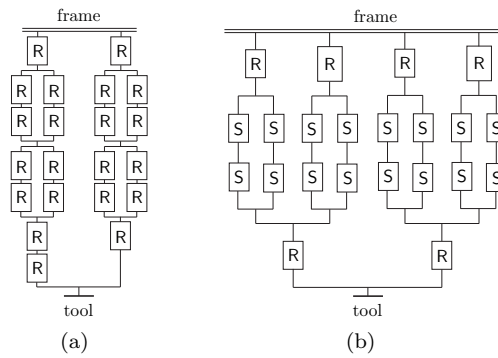


Figure 4. Joint and loop graphs of (a) the McGill SMG, and (b) the H4 robot

8. Conclusions

A formulation capable of measuring the complexity of kinematic chains at the conceptual stage in robot design was proposed in this paper. To this end, the complexity of the six lower kinematic pairs and a formulation of the complexity of kinematic bonds were introduced. Finally, the complexity values of two realizations of the Schönflies displacement subgroup were computed.

Notes

1. Named after the French mathematician Gabriel Lamé (1795–1870), who first introduced these curves.

References

- Angeles, J. (2005). The degree of freedom of parallel robots: a group-theoretic approach. *Proc. IEEE Int. Conf. Robotics and Automation*, 1017–1024.
- Angeles, J. (2004). The qualitative synthesis of parallel manipulators. *ASME Journal of Mechanical Design* 126, 617–624.
- Boyd, S. and Vandenberghe, L. (2004). *Convex Optimization*. Cambridge University Press, Cambridge.
- Chakrabarti, A. (Ed.) (2002). *Engineering Design Synthesis: Understanding, Approaches and Tools*. Springer, UK.
- Company, O., Pierrot, F., Shibukawa, T. and Koji, M. (2001). *Four-Degree-of-Freedom Parallel Robot*. European Patent EP1084802, March 21.
- French, M. (1999). *Conceptual Design for Engineers* (Third ed.). Springer, London; New York.
- Gardner, M. (1965). The superellipse: a curve that lies between the ellipse and the rectangle. *Scientific American*, 213, 222–234.
- Grainger (2005, May). *Internet Catalog*. <http://www.grainger.com>: Grainger.
- Hervé, J. (1978). Analyse structurelle des mécanismes par groupes de déplacements. *Mech. Mach. Theory* 13, 437–450.
- Hervé, J. (1999). The Lie group of rigid body displacements, a fundamental tool for mechanical design. *Mech. Mach. Theory* 34, 719–730.
- Khan, W.A., Caro, S., Pasini, D. and Angeles, J. (2006). *The Geometric Complexity of Kinematic Chains*. Department of Mechanical Engineering and Centre for Intelligent Machines Technical Report. CIM-TR 0601, McGill University, Montreal.
- Oprea, J. (2004). *Differential Geometry and its Applications*. Pearson Prentice Hall, New Jersey.
- Shigley, J.E., Mischke, C.R. and Budynas, R.G. (2004). *Mechanical Engineering Design*. 7th ed., McGraw-Hill, New York.
- Suh, N.P. (2005). *Complexity. Theory and Applications*. Oxford University Press, Oxford.
- Taguchi, G. (1993). *Taguchi on Robust Technology Development. Bringing Quality Engineering Upstream*. ASME Press, New York.